JOURNAL OF MATERIALS SCIENCE: MATERIALS IN MEDICINE 10 (1999) 497–501

The influence of the time-dependent properties of bone cement on stress in the femoral cement mantle of total hip arthroplasty

J. P. G. WHEELER, A. W. MILES, S. E. CLIFT
Department of Mechanical Engineering, University of Bath, Bath, BA2 7AY, UK

An empirically determined formula for the creep behavior of bone cement was incorporated into a validated computer model of a cemented femoral total hip arthroplasty component. The stress patterns in the cement mantle were observed over a period of one week, in one instance where the stem–cement interface was rigidly bonded, and in a second, where it was allowed to slip. Principal stresses and maximum shear stresses were shown to decrease rapidly after loading in both situations, suggesting that the stresses generated were not high enough to cause immediate failure, although they may be significant in the long term.

1. Introduction

Polymethylmethacrylate (PMMA) bone cement has been suggested as a potentially weak link in cemented hip arthroplasties, and its various properties have been the focus of many studies. However, attention has only occasionally been given to a highly significant characteristic, i.e. the visco-elastic behavior of PMMA at body temperature. This term refers to the phenomenon that occurs in many materials, that at high temperatures, strain is no longer a function of stress alone, but also depends on time and temperature. The practical result of this is that under a constant load, strain will gradually increase over time (''creep'') and conversely, at a constant strain, stress will diminish over time (''stress relaxation'') [1]. The typical creep behavior of a material begins with a period of rapid deformation (primary creep), which slows with time until a period of steady state creep is reached (secondary creep), i.e. the rate of elongation remains constant. Beyond this, the creep rate begins to increase again (tertiary creep) until the point of failure is reached [2]. For the remainder of this paper, the term ''creep'' will be used to encompass both classical models of creep and stress relaxation.

PMMA cement, like all other polymers, begins to exhibit visco-elastic behavior as its temperature approaches a level known as the glass transition temperature, T_g. Well above this temperature, polymers become rubbery or fluid; well below it, they are hard and sometimes brittle, and do not creep [3]. T_g for PMMA is approximately 370 °K, and is close enough to body temperature (310 °K) for visco-elastic behavior to become significant [4].

Holm [5] has stated that creep of PMMA cement is a major factor in the long-term performance of cemented total hip arthroplasties. This view has also been put forward by several other authors [6–8]. Numerous authors have conducted finite element investigations into the consequences of a sliding femoral stem–cement interface, although few have shown any comparison with experimental results or any consideration of the effects of stress relaxation, which occurs in bone cement at body temperature. Following earlier work in which finite element models were developed and were shown to produce results matching those of experimental tests, this study examines the consequences of cement creep on well fixed and sliding femoral stems. The finite element analysis package ANSYS 5.0 was used for this work.

2. Method

Verdonschot and Huiskes [6] investigated cement creep under cyclic loading at 38.5 °C and expressed creep strain as a function of the number of loading cycles

$$\log \varepsilon_{creep} = A(\sigma) \log N + B(\sigma) \qquad (1)$$

where ε_{creep} is the creep strain in units of microstrain, N is the number of loading cycles, and A (σ) and B (σ) are functions of the stress level and are defined as

$$A(\sigma) = 0.4113 - 0.1160 \log \sigma$$
$$B(\sigma) = -0.0977 + 1.9063 \log \sigma$$

The response was found to be a typical creep curve of three stages, i.e. a high initial creep rate that slows rapidly, followed by a period of steadily increasing strain and finally accelerating deformation ending in fracture. While this is clearly useful in predicting the life of an implant, it is unfortunately not a standard form of creep equation recognized by the finite element software being used: the ANSYS program provides a number of preprogrammed equations to define creep behavior, but an expression based on number of loading cycles is not among them.

Øysæd and Ruyter [9] also investigated the creep

behavior of acrylic cement, to determine the effect of adding various cross-linking agents. Although creep behavior was not defined empirically, rapid deformation immediately after loading was again reported, followed by a primary creep stage with decelerating creep and then steady state creep.

Chwirut [7] carried out static creep tests at 37 °C on several brands of bone cement, and suggested two relationships to describe creep strain as a function of time and stress. One of these relationships is of a form that may be programmed into the finite element analysis program ANSYS 5.0, i.e.

$$\varepsilon_{cr} = A\sigma^{B}t^{C} \quad (2)$$

where ε_{cr} is the creep strain; σ the stress; t is time; and A, B and C are constants.

The constants A, B and C were reported to be 1.76×10^{-9}, 1.858 and 0.283, respectively, for stress in psi and time in hours. Using Chwirut's values and converting into pascals and seconds, Equation 2 becomes

$$\varepsilon_{cr} = 1.2252 \times 10^{-15}\sigma^{1.8625}t^{0.283} \quad (3)$$

Although this relates to behavior under static loading, it will be shown that it is still useful to describe the behavior of bone cement *in vivo*.

This investigation was based on previous work involving the development of experimentally verified finite element (FE) models of cemented femoral stems implanted in the femur. The models used were axisymmetric, using tapered stems (Fig. 1). One model featured a stem that was perfectly bonded to the surrounding cement mantle, while a second used a stem that was allowed to slip within the cement mantle, using a friction coefficient of 0.2. The two models were compared with experimental work on the basis of hoop strain, and were shown to agree very well, both in the actual values recorded and in the distribution of strain along the length of the models [10]. With the two FE models shown to produce accurate predictions, the models were then updated to include creep behavior in the bone cement.

From the library of creep strain equations available in ANSYS, an equation of the form

$$\Delta\varepsilon_{cr} = C_1\sigma^{C_2}t^{C_3}e^{-C_4/T}\Delta t \quad (4)$$

was selected. Equation 3 was therefore differentiated thus giving the constants $C_1 - C_4$ as shown in Table I.

C_4 was defined as zero to eliminate the temperature term in the equation (since $e^{0/T} = 1$). An axial load of 3 kN was applied to the top of the femoral stem as a uniform pressure, and the temperature of the entire structure was arbitrarily set to 100 K (to avoid the expression $e^{C_4/T} = e^{0/0}$ causing errors). In order to compare the effects of creep at various time intervals with previous models that did not include creep effects, the load was applied as a step load. Results were taken from the models at times after loading of 1 s, 1 and 10 min, 1 and 24 h, and seven days. Results from the earlier models were taken to be equal to the instantaneous response of the structure.

3. Results and discussion

The maximum shear and principal stresses over the duration of the analysis are shown in Table II. Plots of the maximum shear stress in the cement mantle are shown in Figs 2 and 3, illustrating the changes in the stress distribution as well as the reduction in stress.

Fig. 4 shows the drop in stress intensity against time predicted by the ANSYS model over a period of 24 h. The first points shown on the curve are taken from an earlier model in which creep effects were not included [10], i.e. they represent the instantaneous stress state of

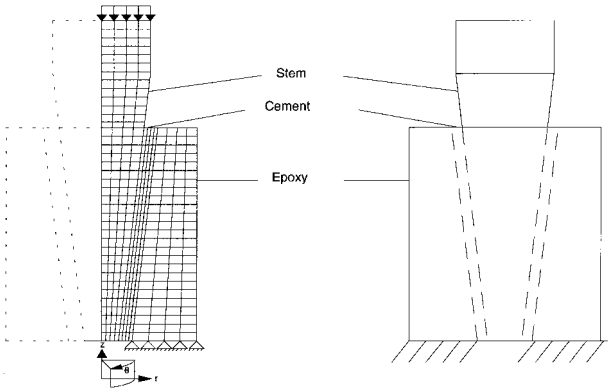

Figure 1 ANSYS axisymmetric finite element model used in the analysis, and the experimental model on which it was based.

TABLE I Creep constants used in ANSYS modeling

Constant	Value
C_1	3.4673×10^{-16}
C_2	1.862 45
C_3	− 0.717
C_4	0

TABLE II Changes in maximum cement stresses over time as a result of creep

Time after loading	Bonded interface		Slipping interface	
	Maximum principal stress (kPa)	Maximum shear stress (kPa)	Maximum principal stress (kPa)	Maximum shear stress (kPa)
No creep	1890	1370	1170	2225
1 s	1510	1055	655	2070
1 min	880	740	211	1270
10 min	642	625	192	1145
1 h	550	580	136	1025
24 h	438	550	20	835
7 days	392	535	20	770

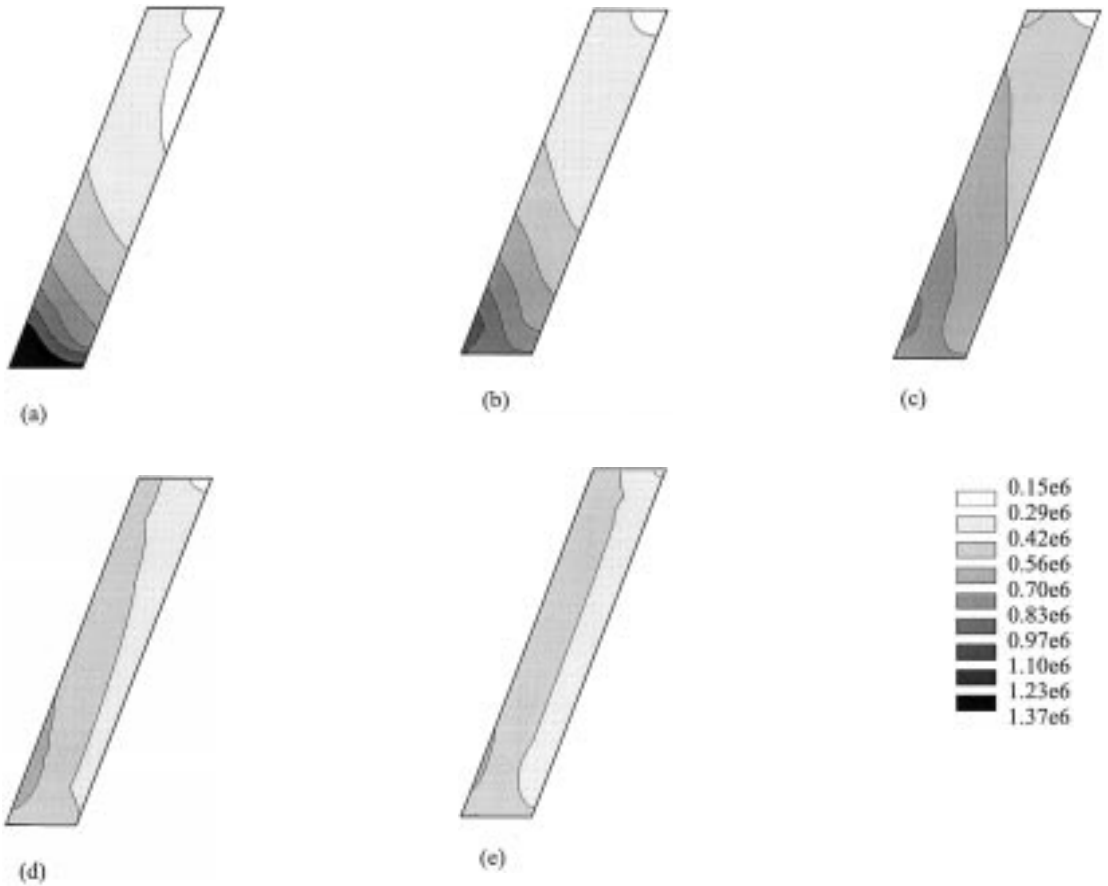

Figure 2 Maximum shear stress in the cement of the bonded model (a) without viscoelastic effects and at (b) 1 s, (c) 1 min, (d) 10 min, and (e) 1 h after loading.

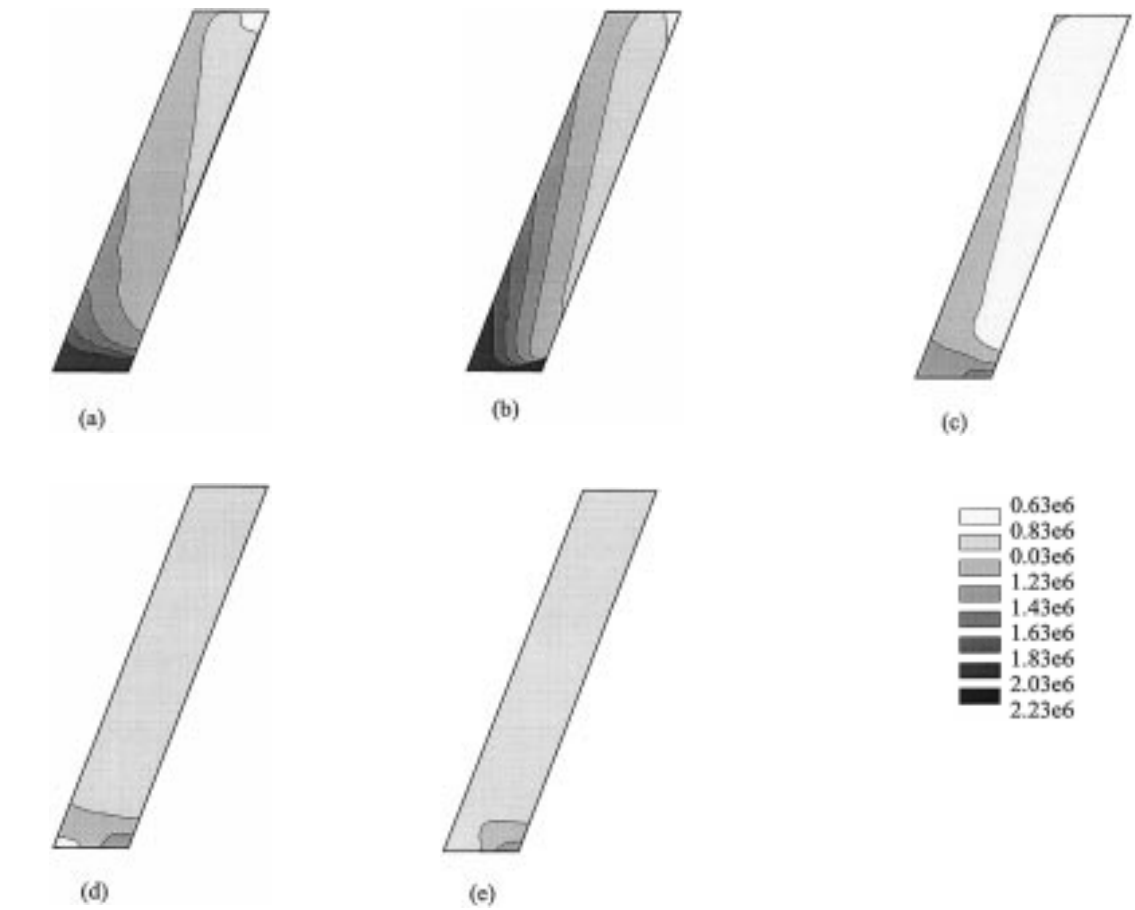

Figure 3 Maximum shear stress in the cement of the slipping model (a) without viscoelastic effects and at (b) 1 s, (c) 1 min, (d) 10 min, and (e) 1 h after loading.

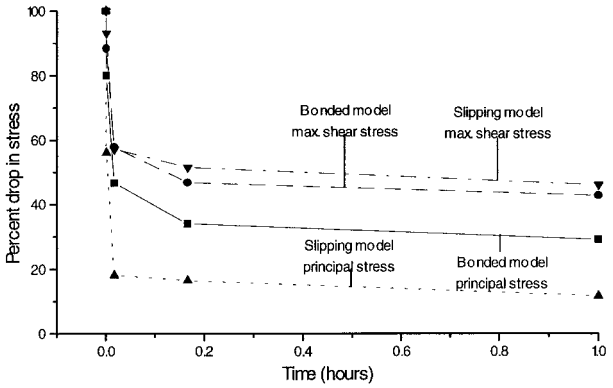

Figure 4 Stress relaxation in the cement mantle of the bonded and slipping models over 1 h.

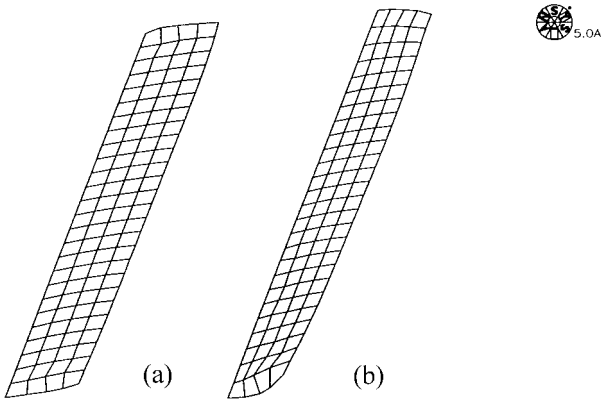

Figure 5 Extrusion of cement after seven days from (a) the bonded model and (b) the slipping model.

the material. The stress dropped most rapidly immediately after loading, as is consistent with typical creep behavior, before levelling out towards a constant value at approximately 1 h after loading. This suggests that even though this is a static analysis, with no dynamic loading applied (e.g. to model walking), the rapid onset of stress relaxation means that these results are very relevant to the behavior of bone cement *in situ*, particularly in the early post-operative stages when patient activity is likely to be low. The rate of attenuation of the peak stresses, falling 40% after only 1 s, supports this.

After one week under continuous load, the maximum shear stress predicted in the cement of the model with the bonded stem–cement interface had levelled out at just under 0.5 MPa, a reduction of 60%. The maximum principal stress had fallen by 79% to 0.4 MPa. However, after only 1 h, the maximum shear stress fell from 1.37 MPa upon loading to 0.58 MPa, a drop of 58%. A drop in maximum shear stress of 12%, and a drop in maximum principal stress of 20% occurred after 1 s under load. This rapid reduction implies that cement fracture is extremely unlikely to be caused by high stresses, and that fatigue damage is by far the major mechanical factor contributing to failure of the cement mantle. In light of the large reduction of stress due to cement creep, it is also suggested that investigations that do not include the effects of creep can only give a limited account of the load transfer, and are likely to give stress predictions far higher than would actually occur *in vivo*. Furthermore, as loading will be applied gradually *in situ* rather than as a single step load, the high stresses predicted by such models are unlikely ever to occur in an implant.

An examination of the distorted shape of the cement mantle after seven days revealed that, as expected, cement had been extruded from both ends of the cement mantle. The plot in Fig. 5 shows a highly exaggerated plot of this extrusion for the purposes of illustration; however, the actual distance extruded by the cement was predicted to be 0.2 mm, i.e. so small as to be almost invisible to the naked eye.

The peak shear stress observed in the slipping model was approximately 60% higher than that in the model with the bonded stem–cement interface. This too was rapidly reduced with the onset of stress relaxation, but remained higher than the non-slipping model. Whether or not this increase may be detrimental to the fixation of the implant depends upon the magnitude and location of the maximum stresses. As the maximum stresses did not occur near the bone–cement interface, they would be unlikely to result in loosening of the implant. Both shear and principal stresses were attenuated more quickly in the presence of a slipping stem–cement interface, presumably as a result of the cement adjacent to the interface being able to move more freely.

The maximum stresses occurring in the cement mantles in both cement models eventually fell by an average of 68%. Although the model with the slipping interface was found to produce higher maximum stresses, the stress levels were still well within the values of ultimate tensile and shear strength reported in the literature, summarized by Saha and Pal [11] (ultimate tensile strength $= 22 - 48$ MN m^{-2}, ultimate shear strength $= 21 - 41$ MN m^{-2}). Given that the stresses in both models fell by approximately 80% of the final total drop after only 10 min of stress relaxation, it therefore appears unlikely that high stress within the cement mantle causes sudden failure of the cement.

4. Conclusions

It is apparent that stresses of the order required to result in sudden failure of the cement mantle are unlikely ever to occur *in vivo*, given the rapid rate of stress relaxation immediately after loading. Although a slipping stem–cement interface initially produces higher maximum shear stresses within the cement mantle than a rigidly bonded interface, these higher stresses are well within the values of ultimate shear stress reported elsewhere, and are unlikely to result in damage to the stability of the implant as they do not occur near the bone–cement interface. Moreover, the stresses in the slipping model were attenuated more quickly than those in the bonded model, probably as a result of the cement adjacent to the interface being able to move more easily. It is therefore indicated that a complete picture of the stress pattern in the implanted femur cannot be achieved without consideration of the creep properties of acrylic bone cement at body temperature.

Acknowledgments

This work was supported by a grant from the Engineering and Physical Sciences Research Council. Thanks to Strucom for the provision of ANSYS 5.0.

References

1. C. HALL, ''Polymer Materials'', (Macmillan, London, 1981) 57.
2. J. BLACK, ''Orthopaedic Biomaterials in Research and Practice'', (Churchill Livingstone, New York, 1988) 65.
3. C. MIGLIARESI, L. FAMBRI and J. KLOARIK, *J. Biomaterials* **15** (1994) 875.
4. A. J. C. LEE, R. D. PERKINS and R. S. M. LING, in ''Implant Bone Interface'', edited by J. Older (Springer-Verlag, London, 1990) pp. 85–90.
5. N. J. HOLM, *Acta Orthop. Scand.* **51** (1980) 727.
6. N. VERDONSCHOT and R. HUISKES, *J. Appl. Biomater.* **5** (1994) 235.
7. D. J. CHWIRUT, *J. Biomed. Mater. Res.* **18** (1984) 25.
8. T. L. NORMAN, V. KISH, K. HUSTOSKY and J. D. BLAHA, *Adv. Engng BED* **26** (1993) 247.
9. H. ØYSÆD and I. E. RUYTER, *J. Biomed. Mater. Res.* **23** (1989) 719.
10. J. P. G. WHEELER, A. W. MILES and S. E. CLIFT, *Proc. IMechE Part H–J Engng Med.* **211H** (1997) 181.
11. S. SAHA and S. PAL, *J. Biomed. Mater. Res.* **18** (1984) 435.

Received 15 September 1995
and accepted 27 August 1998